Journal of Energy Storage 97 (2024) 112963

Contents lists available at ScienceDirect

Journal of Energy Storage

journal homepage: www.elsevier.com/locate/est

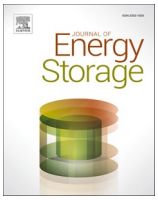

Research papers

Multi-objective optimization of a polygeneration grid including thermal energy storage system

Mario Luigi Ferrari [a,*], Lorenzo Gini [a], Paolo Di Barba [b], Maria Evelina Mognaschi [b], Elisabetta Sieni [c]

[a] Università degli Studi di Genova, Italy
[b] Università degli Studi di Pavia, Italy
[c] Università degli Studi dell'Insubria, Italy

ARTICLE INFO

Keywords:
Multi-objective optimization
Polygeneration smart grid
Thermal energy storage
Heat pump

ABSTRACT

The aim of this work is the optimization of a polygeneration grid including renewable sources and fossil-fuel based prime movers. The system produces both electrical and thermal power and is equipped with a thermal energy storage device in the form of a hot water tank. The grid layout has been chosen to consider the energy needs of the University campus in Savona with a configuration to improve the flexibility for a possible extensive optimization.

Starting from the energy demands of different typical days, a multi-objective approach has been used to minimize both generation costs and CO_2 emissions. The activity has been carried out comparing the use of different technologies (e.g., boiler against heat pump) in order to assess performance in different cases. Special attention has been devoted to an innovative approach for thermal energy storage optimization. Since the sizing of energy storage devices remains an open aspect due to balancing of energy security constraints and cost/emission association to the stored energy, the innovative method proposed here can generate solutions with important benefits on the grid performance and optimization. Moreover, due to possible contrasts of minimization objectives, this work shows the benefits related to a multi-objective approach applied to a real smart grid. An important innovation is the application of a heat pump in grid optimization analyses. In details, the algorithm can demonstrate the improvements in terms of emissions and cost savings considering the innovative integration of existing technologies with the heat pump (−13.2 % cost decrease for the cost minimization target, −16.6 % CO_2 emission decrease for the CO_2 minimization objective, and, finally, −35.2 % for the cost*CO_2 innovative objective proposed here).

1. Introduction

In recent years, the environmental issues [1] coupled to the cost increase of fossil fuels (especially natural gas) [2] generate special attention on the importance of energy management. Although in the past single objective optimization was considered a good solution for minimizing generation costs or maximizing the efficiency [3,4], the recent fuel cost scenario [5] drives the focus to more complex approaches based on multi-objective optimization algorithms [6]. In detail, while an efficiency maximization could be a solution close to the cost minimum, the recent large cost increase makes important to identify also minimum cost solutions [7]. On the other hand, depending on the system configuration and the operative conditions, the minimum cost solution cannot match the minimum CO_2 emission condition. So, a multi-objective energy management system can produce results for the necessary operative choices to optimize a polygeneration smart grid, especially in case of small systems in the tens/hundreds of kilowatt size [8]. While traditionally multi-objective problems are reduced to single-objective using a preference function [9], in this paper, the multi-objective problem is solved in terms of identifying the relevant Pareto front. Instead of using genetic algorithms, the Non-dominated Sorting Genetic Algorithm-II (NSGA-II) approach is applied in this work because it has important flexibility potentialities in case of large number of variables [10,11]. So, an important innovation is the application of an improved version of this algorithm in a polygeneration smart grid

* Corresponding author.
E-mail addresses: mario.ferrari@unige.it (M.L. Ferrari), lorenzo.gini@edu.unige.it (L. Gini), paolo.dibarba@unipv.it (P. Di Barba), eve.mognaschi@unipv.it (M.E. Mognaschi), elisabetta.sieni@uninsubria.it (E. Sieni).

https://doi.org/10.1016/j.est.2024.112963
Received 23 June 2023; Received in revised form 18 June 2024; Accepted 8 July 2024

Nomenclature

Acronyms

CHP	Combined Heat and Power generator
DV	Design Variable
GA	Genetic Algorithm
HP	Heat Pump
mGT	micro Gas Turbine
NSGA	Non-dominated Sorting Genetic Algorithm
PPV	PhotoVoltaic Panel
PV	PhotoVoltaic
TES	Thermal Energy Storage

Variables

A	Area
Achp	Turn on time durations
C	Cost
COP	Coefficient Of Performance
d_{ij}	Euclidean distance
E	Energy
F, f_i, n_f	objective functions
l	load
$\dot{m}$	mass flow rate
n_y, x	variables
P	power
Pb	boiler power
Pchp	microturbine power
R_S	Solar Radiation
SOC	State Of Charge
Tchp	microturbine Turn on time instants
x_a, x_b	feasible solutions
U, u_i	utopia solutions

Greek symbols

Φ	image
Ψ	preference function
σ	parameter

Subscripts

0	initial
CHP	Combined Heat and Power
el	electrical
LG	Local Grid
nom	nominal
th	thermal

equipped with different prime movers, including a heat pump, and energy storage technology. Moreover, in comparison with traditional approaches [12], the whole procedure results in a quick convergence towards the non-dominated region of the objective space.

Since this work incorporates the optimized integration of renewable sources with fossil-fuel based plants, attention is devoted to the existing technology proposing effective feasible solutions for the present energy market [13]. In detail, starting from a configuration similar to the smart grid operating in the University campus located in Savona (Italy) [14], an innovative solution is proposed [15]. Moreover, application of a heat pump [16] has been demonstrated effective by the results obtained with the mentioned energy management system. On the thermal energy side, special attention is devoted to the hot water tank [17]. Although energy storage is a high relevance issue due to the proposal of different technologies (batteries [18], hydrogen [19], ammonia [20], other chemicals for the electrical side), on the thermal side [21] attention is usually focused on advanced systems, such as phase change materials [22,23], thermochemical systems [24], high temperature storage [25], etc. Due to the application type, in this work attention is focused on a standard technology (water tank) considering innovation aspects on the device sizing. In detail, the sizing and management of energy storage systems remain an open issue. This is confirmed by different proposed methods that are not able to finalize the approach for market penetration (e.g. quadratically-constrained mixed-integer programming formulation in [26], multi-objective dynamic optimization model based on long-time data in [27], and model predictive control framework in [28]). This is mainly due to some aspects not completely defined (for instance the cost association to the stored energy is not unambiguous due to the fact that the related energy could have been produced by different prime movers operating with different performance) that moved the authors to propose in this work an innovative approach based on parametric curves. These are based on the initial state of charge (SOC) and the device size to identify the optimal solutions considering different objectives, such as cost and CO_2 emission minimization.

Considering the centrality of the energy storage system, the paper presents the proposed smart grid, the component models (based on experimental data [29] or validated tools [30]) and the related multi-objective optimization algorithm. Then, after the description of inputs/constraints and the parametric curves for storage system sizing, attention is focused on the optimization results. The analysis on the optimization results in terms of cost and CO_2 emission saving demonstrates the effective performance of the proposed approach. Moreover, the results show the benefits of the heat pump application (against the boiler-based layout) for both costs and CO_2 emissions.

2. Polygeneration grid description

The grid layout has been chosen starting from the knowledge (and the benefits) of the smart-grid available on the University campus in Savona [14,15]. However, different component sizes and types were taken into account to investigate more flexibility in the optimization performance and to explore innovative solutions (e.g. for the thermal energy storage sizing). So, the grid was sized for satisfying the electrical and thermal loads of the University campus in Savona [14,15]: although an overnight base load is present due to the student accommodations and the refrigerators/freezers in the campus canteen, the largest part of both electrical and thermal load is related to the campus daily activities (lectures, study/computer rooms, professors' offices, laboratories and canteen/bar buildings). The polygeneration grid of this work is proposed in two different layouts (Fig. 1). In both cases, it includes both electrical and thermal local grids. On the electrical side the system includes a connection to the main energy utility grid (maximum exchangeable power: 1 MW; no selling to the main grid), while on the thermal side hot water pipe circuit is connected to a water tank to be sized in the 250 kWh – 750 kWh range. This range has been chosen to enlarge the 5000 l hot water tank demonstrated essential for optimization at laboratory level [17]. Moreover, the grid includes in both layouts: 77 kW peak-power Photovoltaic (PV) panels, a T100 microturbine in CHP mode (100 kW electrical and 160 kW thermal powers in design conditions, 30 % nominal electrical efficiency, performance maps for the off-design behaviour reported in [29]). The PV panels (17 % efficiency) are installed on the roof of a campus building (south oriented), while the T100 turbine can work in the 20 kW–100 kW range on the electrical side and in the 50 kW–160 kW on the thermal side (thanks to a partial recovery of the exhaust heat content).

Although the two different layouts are quite similar, they include different prime movers on the thermal side. While the layout 1 includes a 150 kW boiler fed by natural gas (a very conventional system [14,15]),

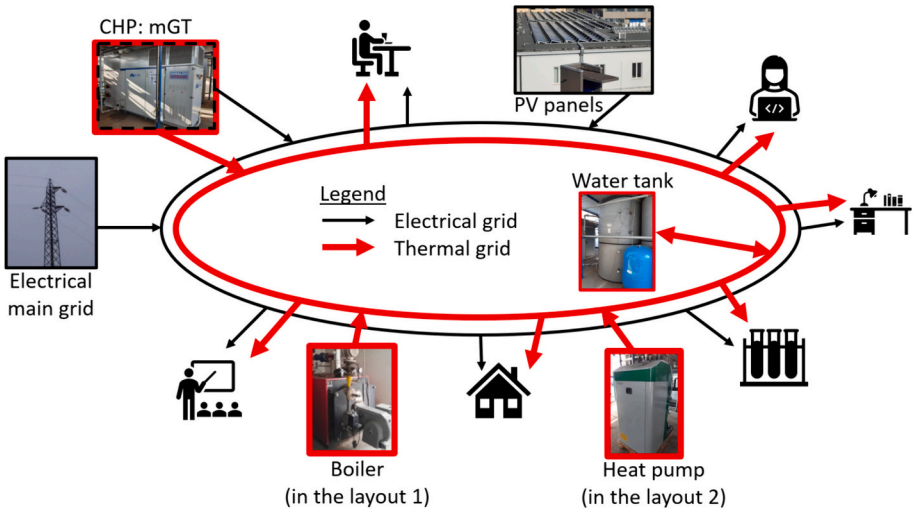

Fig. 1. Polygeneration grid layout including a boiler on the thermal side (layout 1) or a heat pump (layout 2).

in the layout 2 the boiler is substituted by a 75 kW heat pump [31]. Due to typical component characteristics, the boiler is able to operate in part-load operations (in the 15 kW–150 kW range), while the heat pump (3.5 COP) works in on/off mode. This alternative solution has been chosen because, although based on commercial components, it is not fully investigated in smart-grids and its application with a management based on a multi-objective algorithm is innovative.

3. Methodology

Due to the fact that the minimization of the energy cost and CO_2 emission are in contrast objective functions, a multi-objective approach has been considered in this work. The details for the single component modelling are reported in the following subsection.

3.1. Single component modelling

All prime mover models for individual components utilize steady-state approach, incorporating correlations validated in prior research [14]. The T100 CHP model integrates off-design behaviour validated part-load curves, as determined by the University of Genoa at the Innovative Energy System Laboratory (Eqs. (1), (2)) [29]. However, it should be noted that this model does not take into account the thermodynamic internal processes between components. The Eq. (1) and the Eq. (2) show the fuel mass flow and the thermal power as a function of the electrical power.

$$\dot{m}_{fuel\_CHP} = P_{el\_CHP} * a_1 + b_1 \quad (1)$$

$a_1 = 6.22 * 10\hat{}5$ [(kg/s)/(kW)]
$b_1 = 181.12 * 10\hat{}5$ [kg/s].

$$P_{th\_CHP} = P_{el\_CHP} * a_2 + b_2 \quad (2)$$

$a_2 = 1.41$ [kW_{th}/kW]
$b_2 = 10.9$ [kW_{th}].

The boiler model simulates the part-load operations using off-design characteristics taken from literature. The equation below defines the efficiency at part-load operations according to the University of Genoa in-house tool (Eq. (3)) [32], that allows to compute the fuel consumption considering standard value for natural gas LHV. The boiler model replicates part-load operations by employing off-design characteristic curves sourced from literature. Eq. (3), derived from the mentioned in-house tool [32], delineates the efficiency during part-load operations. This equation facilitates the computation of fuel consumption, utilizing standard values for natural gas lower heating value.

$$\eta = \eta_{nom} * \sqrt{(1 + l_{\%})/2} \quad (3)$$

The PV electrical power is computed according to Eq. (4), as a function of the solar radiation, the PV surface and the efficiency that is set and equal to 17 % according to literature value [33]. The calculation of PV electrical power follows Eq. (4), which is contingent upon solar radiation (R_S), PV surface area (A_{PV}), and efficiency (η_{PV}).

$$P_{PV} = R_s * A_{PV} * \eta_{PV} \quad (4)$$

Finally, the heat pump model operates in a binary on/off manner and therefore does not incorporate part-load coefficient of performance (COP) correlations. Additionally, the thermal energy storage is assumed to be adiabatic, with heat exchange losses neglected.

3.2. Multi-objective formulation of an optimization problem

In some cases, multiple objective functions are simultaneously prescribed. Problems of this kind are the so-called multi-objective or multi-criteria optimization problems. In electrical engineering, many design problems are characterized by a vector of n_f objective functions in mutual conflict, for which the most general solution is represented by non-dominated solutions, which belong to the Pareto front. A non-dominated solution is a solution for which the decrease of a function is not possible without the simultaneous increase of at least one of the other functions.

Formally, considering n_v variables, a multi-objective or multi-criteria optimization problem can be defined as follows (Eq. (5)):

$$given\ x_0 \in \Omega\ \text{find}\ \inf_x F(x),\ x \in \Omega \quad (5)$$

where x_0 is the initial solution, $F(x)$ the objective function and Ω is the feasible region.

In general, a multi-objective optimization problem is subject to constraints (Eq. (6)). In detail, g_j and h_j are general constraint functions.

$$\begin{aligned} g_j(x) &\le 0 \quad j = 1, \ldots, n_i \\ h_j(x) &= 0 \quad j = n_i + 1, \ldots, n_c \end{aligned}$$

$$\ell_k \le x \le u_k \quad k = 1, \ldots, n_b \quad (6)$$

In Eq. (5), $F(x) = \left\{ f_1(x), \ldots, f_{n_f}(x) \right\} \subset R^{n_f}$ is the objective vector, assuming $n_f \ge 2$.

With reference to the optimal scheduling problem, typical examples of $f_i(x)$ functions could be the energy cost or production of CO_2 related to the power generators. While the design variables could be the time

instants of turn-on and turn-off of the electrical energy generators as well as their power regulation and also the heat pump turn-on or turn-off and the boiler regulation. In turn, possible constraints could be related to the equipment scheduling time because an operation cycle must terminate before restarting a new one.

Therefore, F defines a transformation from the design space R^{n_v} to the corresponding objective space R^{n_f}. It is assumed that the objectives are bounded and they are in mutual conflict (Eq. (7)):

$$\exists x_i^* \text{ such that } f_i(x_i^*) = inf f_i(x)\ ,\ i = 1,\ldots,n_f \tag{7}$$

and $x_i^* \neq x_j^*\ ,\ i \neq j\ ,\ j = 1,\ldots,n_f$.

In general, the so-called Utopia solution is defined as [34] (Eq. (8)):

$$U = \{U_i\} = \{\, inf\, f_i(x)\,\},\ i = 1,\ldots,n_f. \tag{8}$$

It minimizes all f_i functions simultaneously, and it does not exist. It can be noted that the Utopia point U is out of the feasible design region Y (Fig. 2a). In a symmetrical way, the Anti-Utopia point A (see Fig. 2a) can be defined as the solution which simultaneously maximizes all f_i, while the Nadir point R is the mirror image of the Utopia point [35].

In this frame, given two feasible solutions $x_a \in \Omega$ and $x_b \in \Omega$, x_a is said to dominate x_b if $f_i(x_a) \leq f_i(x_b), i = 1,\ldots,n_f$ and $f_i(x_a) < f_i(x_b)$ for at least a value of $i = 1,\ldots,n_f$. Now, let $P \subset \Omega$ be a set of non-dominated solutions $\tilde{x}_a$; if, for any $\tilde{x}_a \in P$, there is no $x_b \in \Omega$ dominating $\tilde{x}_a$, then P represents the Pareto set and the corresponding image $\Phi = F(P)$ is the Pareto front; the latter is also called trade-off curve.

For the sake of an example, in Fig. 2b six solution points and the dominance dihedral related to solution y_1 are shown in a two-dimensional space (y_3), which belongs to the dominance dihedral, dominates y_1, while y_2, y_4 and y_6 are indifferent with respect to y_1 and, finally, y_5 is dominated by y_1.

Traditionally, the multi-objective problem is reduced to a single-objective one by using a preference function $\psi(x)$, e.g. the weighted sum of $f_i(x)$ (Eq. (9)):

$$\psi(x) = \sum_{i=1}^{n_f} c_i f_i(x)\ ,\ 0 < c_i < 1\ ,\ \sum_{i=1}^{n_f} c_i = 1 \tag{9}$$

However, the selection of the c_i coefficients is arbitrary and gives rise to a particular solution only. So, in the last decades, attention is paid to methods able to solve a multi-objective optimization problem according to Eqs. (5)–(8); more recently, new methods for solving the so-called many-objective optimization problems (more than two or three objective functions) have been proposed [36–38].

Accordingly to this section, the multi-objective problem is solved in terms of identifying the relevant Pareto front, i.e. the set of non-dominated solutions.

3.3. Optimal scheduling problem

The study proposes an optimal scheduling approach for pre-existing micro-grids, emphasizing the benefits of incorporating thermal energy storage. The optimized energy management facilitated by storage utilization and its appropriate sizing stand as a significant contribution. So, the integration of construction costs for all prime movers is important for the component sizing when it is necessary to start from the installation activity of all the prime movers. Although this was already considered in previous works [32,33], this paper focuses attention on the grid management with multi-objective approach and an innovative method for the thermal storage integration.

The optimization problem considers two different cases:

- Case 1: one CHP that can be activated two times in 24 h with at least 2 h of turning on at a fixed percentage of the rated power and one boiler that can be tuned every 2 h in the 24 h.
- Case 2: one CHP that can be activated two times in 24 h with at least 2 h of turning on at a fixed percentage of the rated power and one heat pump that can be turned on or off every 2 h.

The design variables consider a time window lasting 24 h; they are defined as follows:

- Turn on time instants of the CHP, $Tchp_j$, j = 1,2.
- Turn on time duration of the CHP, $Achp_j$, j = 1,2.
- Rated-power percentage of the CHP, $Pchp_j$, j = 1,2;
- Twelve rated-power percentages for the boiler, Pb_i, $i = 1\ldots12$ (only layout 1 case);
- Twelve time-instants of turn on/turn off for the heat pump, HP_k k = 1…12 (only layout 2 case).

To complete the problem definition, Table 1 reports the number of design variables and the range of variations for the considered design variables for the two considered cases.

The objective functions consider the tuning of all the electrical and thermal sources in the smart grid in order to satisfy the requested thermal and electrical load in an average day of a given month (e.g. November). They are the energy cost, f_1, and the production of CO_2, f_2, to be minimized (Eqs. (10)–(11) - where C, E, $\dot{m}$ and P stands for cost, energy, mass flow and power respectively).

$$f_1 = \sum_{k=1}^{24} \left[C_{fuel} \left(\dot{m}_{fuel_{CHP}}(k) + \dot{m}_{fuel_{boiler}}(k) \right) + C_{el_{LG}}(k) P_{el_{LG}}(k) \right] \tag{10}$$

$$f_2 = \sum_{k=1}^{24} \left(E_{CO2_{CHP}} P_{el_{CHP}}(k) + E_{CO2_{boiler}} P_{th_{boiler}}(k) + E_{CO2_{LG}}(k) P_{el_{LG}}(k) \right) \tag{11}$$

The design variables related to the CHP are subject to the following constrains (the parameter definition for these variables is reported in the points above).

- $Tchp_2 > Tchp_1$
- $Tchp_1 + Achp_1 < 24$ and $Tchp_2 + Achp_2 < 24$
- $Tchp_1 + Achp_1 < Tchp_2$

In detail, the second turn-on of the CHP has to be subsequent to the turn-off of the previous functioning cycle and the CHP functioning time must not exceed the 24 h. Following a criterion of penalty technique, if

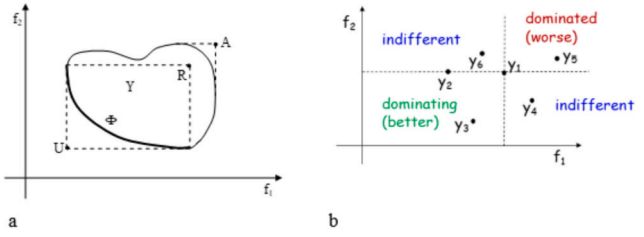

Fig. 2. Objective space (a) and Pareto dominance criterion (b).

Table 1
Design variables (DV) for the two cases, and corresponding variation ranges (the column titles are explained in the section text – in the points related to the design variables).

	# DV	$Tchp_j$	$Achp_j$	$Pchp_j$	Pb_i i = 1,2,11,12	Pb_i $i = 3,\ldots10$	HP_k
Case 1	18	[1, 24]	[2, 20]	[0.3, 1]	[0, 0.2]	[0.2, 1]	–
Case 2	18	[1, 24]	[2, 20]	[0.3, 1]	–	–	0 or 1

the DV does not satisfy the constraints, the objective functions are set to 10^{15}.

Traditionally, the optimal scheduling of electric and thermal sources is approached by means of techniques of linear programming, due to the substantially high number of the degrees of freedom ruling the turn-on and turn-off cycle of each generator in the time frame. More recently, stochastic optimization methods have been applied to this kind of scheduling problems. A few of them are Wind Driven, Particle Swarm, Cuckoo Search, Genetic Algorithms, Grey Wolf Optimizer [39–43].

In general, the aim of the optimization problem is the reduction of the cost of the system or the reduction of pollutant emissions or the reduction of the peak load. In the literature, these goals are formulated in terms of objective functions which, in turn, are incorporated in a single preference function by means of a set of weight coefficients as in (5). However, this approach is somehow limiting due to the arbitrary choice of weights, while the most general solution is represented by the set of non-dominated solutions.

3.4. Optimization algorithm

In the last decades, different optimization techniques inspired by nature have been investigated. Genetic algorithms (GA) are a very useful and widely studied optimization techniques; in particular, one of the most used algorithms is the Non-Dominated Sorting Genetic Algorithm NSGA-II [12]. GAs work very well when the number of design variables is low e.g. lower than 10; so, they are commonly used in multi-objective optimization of e.g. electrical machines and electromagnetic devices, because these problems are characterized by a few design degrees of freedom. In this paper, the NSGA-II is applied to a scheduling problem, which is usually characterized by many parameters, depending on the problem formulation.

In GA optimization, a population, which is a set of individuals, is evaluated at each iteration (generation) in terms of rank and crowding distance. The population is ordered in terms of Pareto front and sub-fronts and a rank is assigned to each front: the solutions belonging to the Pareto front have the lowest rank (e.g. rank = 1) while higher ranks are assigned to dominated sub-fronts. For each solution belonging to a given front, the crowding distance is calculated: the solutions aggregating in a cluster are characterized by a crowding distance value lower than isolated solutions. Taking into account the crowding distance helps in obtaining regularly spaced i.e. not clustered solutions in the objective space. The individuals of the current population are ordered first by rank index and then, among each front, by the crowding distance. The best (fittest) individuals are the ones characterized by a low rank and high crowding distance.

In order to create the next generation, highly-fit individuals of the current iteration are combined by a crossover operator to produce offspring. Meanwhile, to increase variation in the search space, a mutation operator is performed at a certain probability level. The generated offspring solutions are added to the current population. Supposing the population size is N, the current population size will be 2*N, since the offspring solutions are added to the current population. Then, the current population is sorted using non-dominance and crowding distance and truncated to N individuals. In this way, the next generation population has size N. This process continues until the stopping criterion, usually a maximum number of generations, is met.

More specifically, the fitness value is assigned to each individual as presented below.

Fitness assignment - Considering a population of $n_p > 1$ individuals, each having $n_f > 1$ objective function values, a non-dominated set of solutions is based on the following procedure.

i) begin with $i = 1$;
ii) for $j = 1$, n_p and $j \neq i$, compare solutions x_i and x_j according to the definition of dominance applied to all n_f objectives;
iii) if, for any j, x_i is dominated by x_j, mark x_i as "dominated";
iv) if all solutions in the population are considered, go to step v;

1. else set i as i + 1 and go to step ii;

v) all solutions that are not marked as "dominated" are non-dominated solutions;
vi) end

All the non-dominated solutions so determined are assumed to identify the first non-dominated front in the populations and are assigned a large fitness value (e.g. equal to n_p). The same fitness value is assigned to all non-dominated individuals in the front to give them an equal reproductive potential. In order to maintain diversity in the population, the non-dominated solutions are then shared with their fitness values. Basically, sharing is achieved by dividing the fitness values by a quantity (called niche count) proportional to the number of individuals around it. This procedure causes multiple optimal points to co-exist in the population. The worst shared fitness value in the solutions of the first non-dominated front is kept for reuse.

After sharing, non-dominated individuals are ignored temporarily to process the rest of population members. This step-by-step procedure is iterated to find the second front of non-dominated solutions in the population. Once they have been identified, a fitness value, which is slightly smaller than the worst fitness value occurred in the previous front, is assigned. Thereafter, the sharing procedure is performed among the solutions of the second non-dominated front, and shared fitness values are found as before. The process is continued until all population members are assigned a shared fitness value.

Sharing procedure – Given a set of n_k solutions (individuals) in the k-th non-dominated front, each having a fitness value f_k, the sharing procedure is performed in the following way for each solution $i = 1,n_k$.

i) Given the i-th solution x_i, the algorithm computes the Euclidean distance d_{ij} with solution x_j in the k-th non-dominated front (Eq. (12))

$$d_{ij} = \sqrt{\sum_{p=1}^{n_v} \left[\frac{x_{ip} - x_{jp}}{x_{up} - x_{\ell p}}\right]^2} \ , \ i \neq j \ , \ j = 1, n_k \tag{12}$$

where n_v is the number of variables, n_k is the number of solutions in the k-th front, [x] is the current set of individuals (actually, a $n_k \times n_v$ matrix), while x_{up} and $x_{\ell p}$ are upper and lower values of p-th columns in [x] matrix, respectively;

ii) d_{ij} is compared with a prescribed parameter σ and the sharing function $s(d_{ij})$ is computed (Eq. (13)).

$$s(d_{ij}) = 1 - \left(\frac{d_{ij}}{\sigma}\right)^2 \text{ if } d_{ij} \leq \sigma, i \neq j, \ j = 1, n_k \tag{13}$$

$s(d_{ij}) = 0$ otherwise.

iii) set j as j + 1: if $j \leq n_k$ go to step 1 and update d_{ij}; else update the niche count m_i for the i-th solution (Eq. (14)).

$$m_i = \sum_{j=1}^{n_k} s(d_{ij}) \ , \ i \neq j \tag{14}$$

iv) update fitness f_k of i-th solution in the k-th non-dominated front to calculate the shared fitness $\widetilde{f}_k$ as follows (Eq. (15)).

$$\widetilde{f}_i = \frac{f_k}{m_i} \ , \ i = 1, n_k \tag{15}$$

v) find the smallest value of $\widetilde{f}_i$ in the k-th front for further processing: the fitness of (k + 1)-th non-dominated front is set as (Eq. (16))

$$f_{k+1} = \inf_{i=1,n_k} \widetilde{f}_i - \varepsilon_k \tag{16}$$

where $\varepsilon_k > 0$ is small enough.

The sharing procedure is characterized by parameter σ; heuristically, it can be set as in Eq. (17).

$$\sigma \approx 0.5 n_q^{-n_v^{-1}} \tag{17}$$

where the integer $n_q > 1$ is the desired number of different non-dominated solutions.

As far as constraint processing is concerned, the constraint-dominance principle is resorted to: solution a constraint-dominates solution b, if any is true:

- a is feasible and b is not;
- a and b are both unfeasible, but a exhibits a smaller constraint violation;
- a and b are both feasible and a dominates b.

The whole population is then reproduced depending on the shared fitness values: since individuals in the first front have better fitness values than solutions of any other front, they always get more copies than the rest of the population. The rationale is to search for non-dominated regions, which will finally lead to the PF. The whole procedure results in a quick convergence towards the non-dominated region of the objective space; the sharing procedure, in turn, helps to distribute individuals over this region.

A drawback of the algorithm is the lack of memory, i.e. the lack of an active use of the solution history. In detail, in a future generation, an unnecessary waste of runtime could occur in evaluating the problem objectives for an individual which is very similar – or equal – to one evaluated in the past. Typically, this happens towards convergence: a possible remedy is to keep track of all the individuals already evaluated, to avoid a time-consuming re-evaluation of objectives.

4. Results and discussion

An essential input regards the energy demands to be considered for this analysis. To have a good compromise between different seasons and to start from conditions that require a significant thermal load, the demands of a working day in November 2021 have been chosen (Fig. 3) [44,45]. However, to have reasonable thermal demand values to be satisfied by the proposed prime movers, the loads considered in this work are the half of the actual demand values of the campus. In details, it is visible a large early morning peak to have comfort conditions for the beginning of the classes in the morning and bar services (at about 8:00). On the electrical side, the demand shows a slow increase up to the day central hours when the campus has the maximum amount of activities. Then, differently from a residential district, the evening load of student accommodations is quite negligible in comparison to the demands of the class time. So, no evening peak is present.

From the economic input point of view, 114 €/MWh has been considered for natural gas, to represent a typical cost situation of the 2021 year [46]. Moreover, variable electricity costs (as in Fig. 4) have been implemented. The case study does not include the power to grid possibility of the microgrid. Due to an important impact of solar PV panels in the Italian energy mix (+5.3 % in 2020 in comparison with the previous year [45]), the CO_2 emissions show a significant decrease (about 20 %) in the midday hours. Although these data are quite variable during the ongoing months, a similar behaviour in the optimization results can be obtained in case of a significant cost increase of both fuel and electricity. On the other hand, the changes for the CO_2 emission point of view are affected by the energy mix changes that are significant during the last decade [45].

4.1. Thermal storage tank

The methodology presented is also an innovative procedure for sizing the thermal storage tank to minimize energy costs and CO_2 emissions. The size range of the thermal storage tank has been selected considering the available space for a hot water tank in typical boiler rooms of a university campus. For sure, larger size solutions can be considered with a further increase of required space and capital costs. So, to avoid complete redesign of campus infrastructures, the 250 kWh – 750 kWh range has been chosen in this work. Moreover, the initial State of Charge (SOC) was considered equal to 0, 50 % or 100 % of the device capacity as first guess value for optimization. Since the thermal storage tank has 3 possible combinations of SOC and size, 250, 500 and 750 kWh, 9 different combinations could be identified. Considering that day-by-day demand variations are usually in the ±5 % range or lower (e.g., extending the analysis to the working days in a week), the impact in the thermal storage sizing is not significant (weekend and holiday days are not taken into account due to very low demands in comparison with the prime mover sizes). Moreover, the initial SOC optimization performed on the entire period (e.g. the proposed 5 working days) can produce an intermediate solution that is not optimal for the mentioned days. So, it is considered preferable to repeat the optimization with the real demands for each day, that, due to the limited variation, is limited to changes in the range of few percentage points. Finally, it is important to highlight that when the final SOC is very different from the optimal initial SOC of the next day, a minimum connection period (e.g., 1 h) could be included between the days (e.g., for recharging operation). For this reason, the

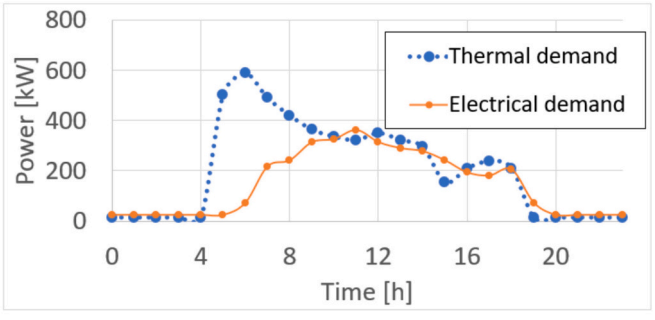

Fig. 3. Thermal and electrical demands for the late autumn case (a day in November 2021).

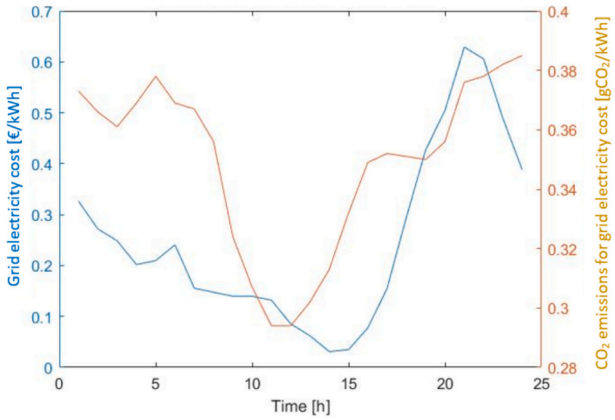

Fig. 4. Electricity cost and CO_2 emission for a reference autumn day in 2021.

SOC difference between the initial and the final condition is carefully taken into account in the analysis of the global system performance (e.g., if at the end of the day the SOC is lower than the value at the beginning, additional cost and CO_2 emissions associated to the recharging are taken into account, as proposed in [17]).

The case study considers an existing smart grid that includes a PV source, a CHP with two tuneable working intervals (with 3 parameters for each turn on: a turn on time, a turn-on time interval, and a working-percentage with respect the maximum capacity), the power grid connection just for buying electricity and a couple of devices (thermal storage tank, heat pump or boiler). Since the thermal storage tank has 3 possible sizes and 3 possible SOC, then two 9 different combinations could be identified for each case study. For each case study a multi-objective optimization was performed in order to identify the design variables that include the CHP working parameters, and the turning on interval for the heat pump or the boiler and working-percentage with respect to the maximum available for the boiler. The range of variations for the design variables are in Table 1. The objective functions were focused to be minimized are the energy cost and CO_2 emission.

The two sets of 9 multi-objective optimization results, one for thermal storage tank-heat pump coupling and one for the thermal storage tank-boiler coupling, were resumed in two parametric curve plots. The calculations have been performed for each case considering the combinations of three different initial state of charge (0, 50 and 100 % as first guess) and three different tank sizes (250 kWh, 500 kWh, 750 kWh). Although, it could be possible to increase the optimization cases, with this approach it is possible to obtain a good compromise between the calculation time and the system performance to be equipped with this tank. In many cases, the optimization process gained the solution for a value of the initial state of charge different from the first guess, considering the constraints: energy balance and the SOC always in the 0–100 % range. For instance, if the solution would present the state of charge lower than zero in the daily scheduling, the following optimization for the same condition would consider a greater initial state of charge.

The global value of Cost, CO_2, Cost*CO_2 have been presented in Figs. 5 and 6, highlighting the Pareto fronts and showing the improved solution for each objective function (Cost, CO_2, Cost*CO_2) corresponding to a set of design variables. Considering that cost and CO_2 emission minimization could be in contrast and generate alternative solutions, the Cost*CO_2 objective function has been considered to have a possible compromise with a simple approach. Thanks to the minimization of this product, it is possible to produce solutions with significant decrease in performance for both costs and CO_2 emissions. For each couple (SOC, Capacity of the TES) of initial conditions for the TES, the best Pareto front has been considered in Figs. 7 and 8 according to the three

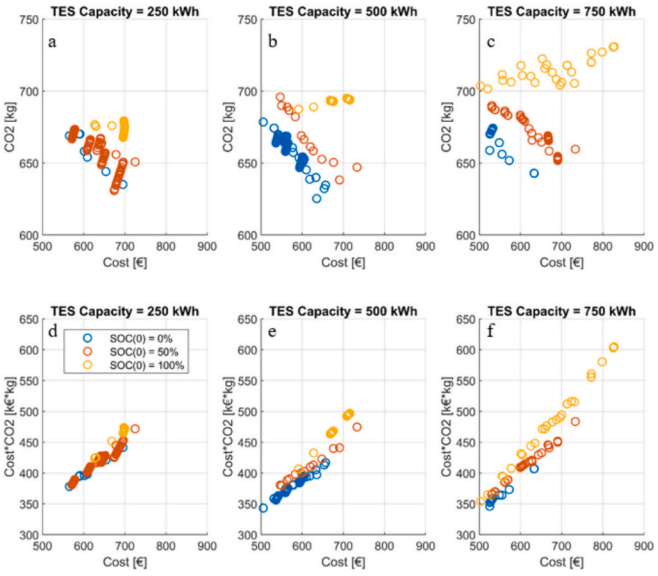

Fig. 6. Pareto front for micro-grid with heat pump.

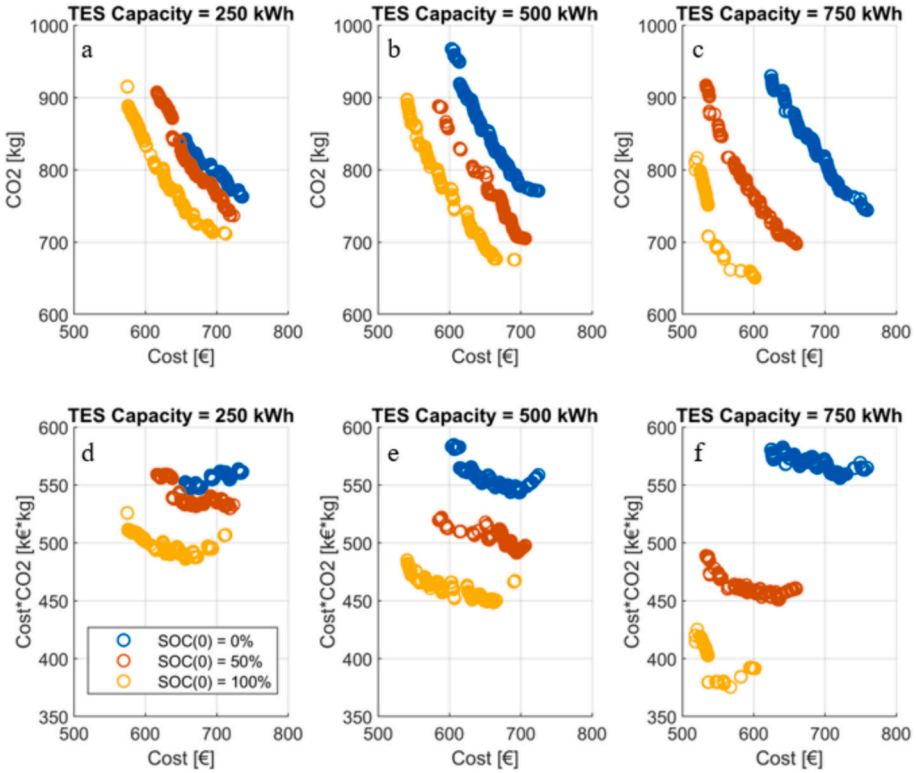

Fig. 5. Pareto front for micro-grid with boiler.

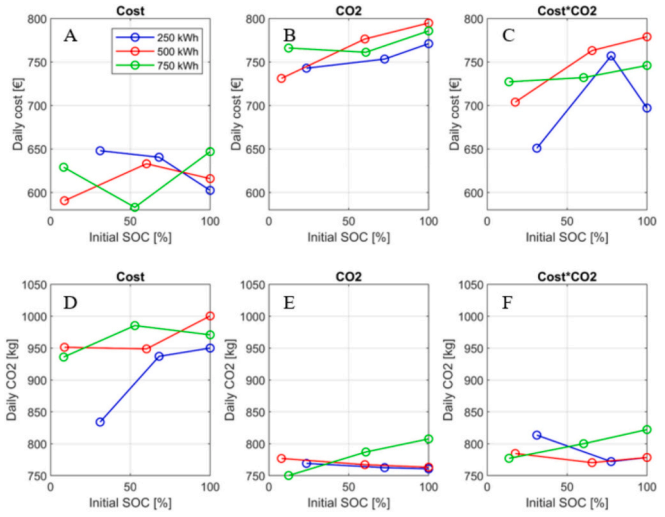

Fig. 7. Parametric curves for sizing the thermal storage tank (boiler case).

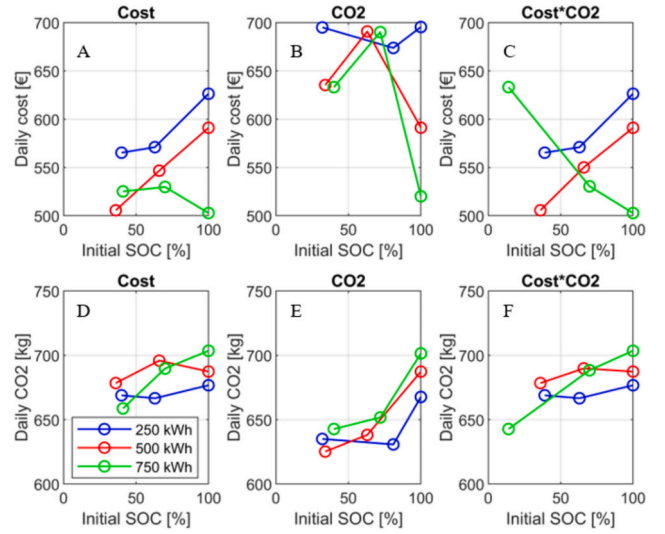

Fig. 8. Parametric curves for sizing the thermal storage tank (heat pump case).

different objective functions Cost, CO_2, Cost*CO_2.

4.2. Polygeneration micro-grid

The obtained solutions were analysed in terms of daily scheduling for each prime mover. The plots (Figs. 5 and 6) show the 100 optimized solutions in each Pareto fronts for the inputs data combinations for both boiler and heat pump cases, highlighting the double objective problem in scatter plots. Each point on the Pareto graph represents an energy scheduling, while the parametric curves enable the identification of optimal outcomes scientifically. Starting from all the produced management solutions, this approach reduces the number of cases and facilitates a streamlined comparison among the most promising energy scheduling options. Although the potential for offering additional energy scheduling options in the case study, the significance of the work lies in deterministically identifying a select few solutions for preferential consideration and ultimately selecting the best among them.

The boiler case results present the product between the two objectives (cost and CO_2) almost constant in the Pareto front, while in heat pump case results the product is proportional to the cost while the CO_2 factor has secondary effect. The Pareto fronts of the boiler are well-defined and present a wide diversity of results, compared to the heat pump case study in particular for CO_2 emissions.

The results, obtained with the proposed innovative method for these kinds of systems, show that the NSGA-II approach has important flexibility potentialities in case of large number of variables (18 in this work). So, although in this work the number of variables is not very high in comparison with the cited limit for the GA (10 variables), the obtained results show the effectiveness of this approach considering also applications in more complex systems (e.g., with additional generators or energy storage devices).

The Figs. 7 and 8 show the results related to the energy costs (first row plots) and CO_2 emissions (second row plot). The panels A and D represent the solution with the minimum of the energy cost, and panel B and E the solution with the minimum of CO_2 emission function. Finally, panels C and F represent the solution for which the product of the two objective functions is minimum (third column with the label "Cost*CO2" in Figs. 7 and 8). With this approach it is possible to combine the obtained solutions to show the best compromise between the two objectives, that for boiler case study is 250 kWh hot water tank starting at 31 % SOC at the beginning of the analysed day (the tested initial SOC, first guess, were 0, 50 and 100 %). This refers to the hour-by-hour results reported in Fig. 11. The best compromise for heat pump case is 500 kWh hot water tank, starting at 36 % SOC at the beginning (Fig. 13). These solutions minimize both cost and CO_2 emissions. In Figs. 7 and 8, the minimum values of the initial SOC are greater than first guess values (0, 50 and 100 %) such that the simulation has reached convergence respecting the constraints in SOC and energy balance. The optimized solutions were analysed one by one to evaluate their feasibility (some solutions were discarded when not respecting the energy balance or the SOC constraints).

The differences between the plots in Figs. 7 and 8 highlight the importance of using a multi-objective approach equipped with NSGA-II for operating with a large number of variables. Moreover, the results show the importance of developing a compromise objective function, such as the innovative Cost*CO_2 product proposed here. Due to contrast conditions for the minimization of the simple objective functions, the combination proposed here is an innovative possible compromise considering a simple computational approach.

Finally, the improvement related to the integration with a heat pump is clear from these results because the curves reported in Fig. 8 show important cost and emission decrease for all the cases. So, the innovation coming from the switching to the layout 2 (the heat pump case) can be confirmed by significant economic and environment benefits.

The final figures (Figs. 9–13) present the daily scheduling hour-by-hour of the polygeneration micro-grid operation, highlighting the splitting of thermal and electrical power generation between the different prime movers (CHP, PPV, Electrical grid, boiler, heat pump), and the state of charge of the energy storage system. In all cases, the electrical generation with PV panels is the same and has the priority over the other sources. These results show that, for the cost optimization objective, the electrical grid contribution is very important, especially for the boiler case. In detail, in Fig. 9 the demands are mainly covered by the grid (electrical side) and by the boiler + the TES (thermal side). This few utilizations of the CHP (e.g. when the electrical energy cost is high) needs to be carefully considered because it reduces the cost justification for the CHP installation. On the other hand, for the CO_2 emission minimization cases (Figs. 10 and 13), the CHP utilization is essential to save fuels (and CO_2 emissions) with the thermal energy harvesting.

Also these results show the importance of the multi-objective approach performed with the NSGA-II algorithm (innovative for these kinds of systems) because the minimization of costs and CO_2 emissions produces different results. Compromise results are obtained with the objective function based on the product (cost*CO_2), as visible hour-by-hour (Figs. 11 and 12). In both cases, an intermediate solution was obtained as visible for the CHP point of view. It is important to highlight that for the heat pump cases, the optimal cost solution and the results related to the cost per CO_2 emission product regards a same hour-by-

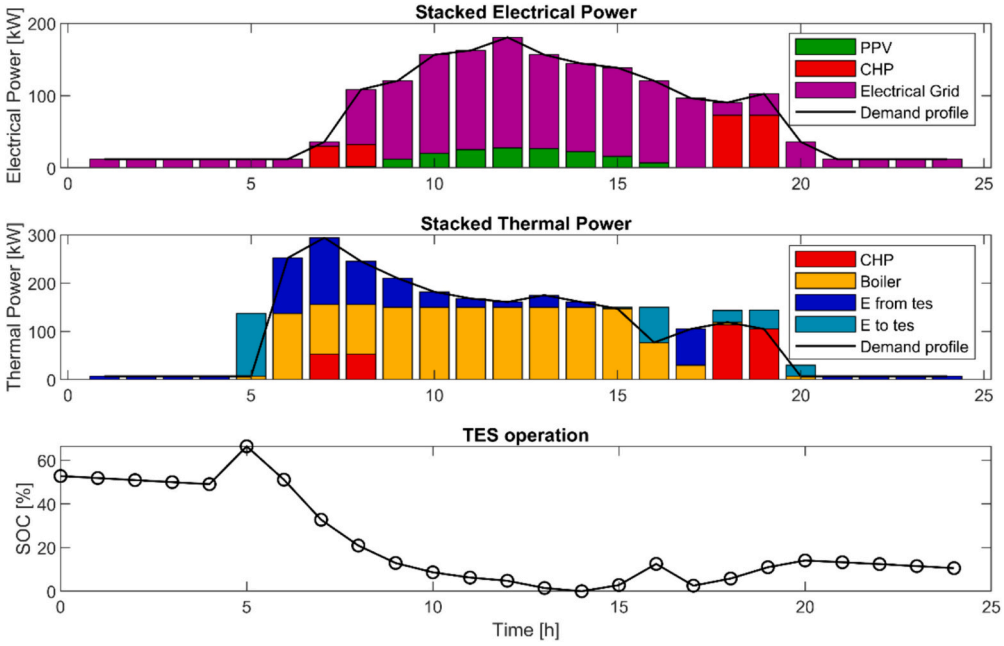

Fig. 9. Daily scheduling: boiler case for the optimal cost solution (SOC(0) = 53 %, Capacity = 750 kWh).

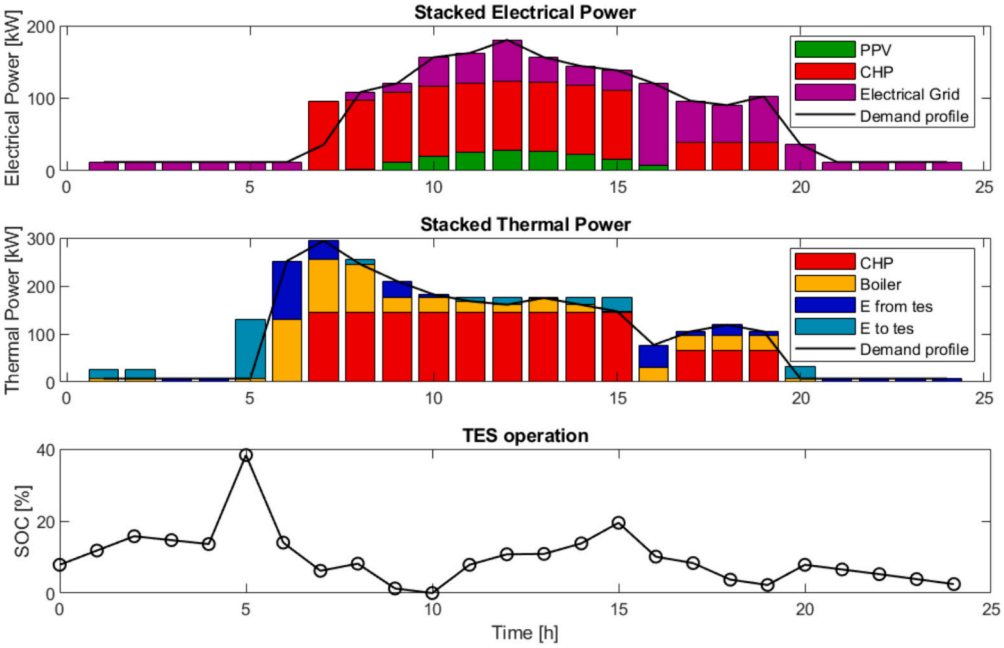

Fig. 10. Daily scheduling: boiler case for the optimal CO_2 emission solution (SOC(0) = 12 %, Capacity = 750 kWh).

hour plot because the best solution is the same Pareto.

An important comparison of global performance is reported in Table 2 for all the six cases. In agreement with the optimization objectives, the minimum values are obtained for the devoted target case (e.g. the minimum costs are obtained for the cost optimization objective). Moreover, it is important to highlight that the benefits of the heat pump application is evident for both costs and CO_2 emissions because the Boiler/HP comparison is always in favour of the heat pump application (−13.2 % cost decrease for the cost minimization case, −16.6 % CO_2 emission decrease for the CO_2 minimization case, and −35.2 % of cost*CO_2 for the case related to the minimization of this product). In detail, the important decrease of the proposed innovative parameter (cost*CO_2) is a result that highlights the benefit of the heat pump application, especially in compromise situation between the cost and the emission minimization.

5. Conclusions

This paper regards the optimization scheduling of a polygeneration smart grid using a multi-objective algorithm. The system includes both electrical and thermal demand/generation and possible energy exchange with the main grid for the electrical side and with an energy storage device (hot water tank) for the thermal side. The multi-objective approach is an important option for the energy management because the minimization of costs and emissions could be in contrast in some operative conditions. Moreover, an innovative approach for thermal energy

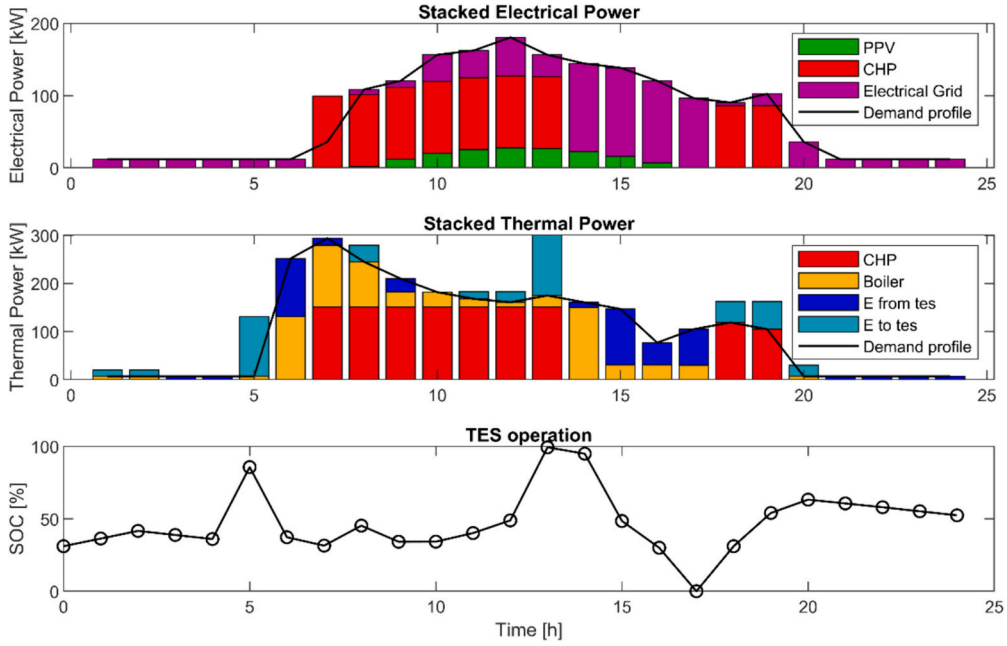

Fig. 11. Daily scheduling: boiler case with the optimal cost*CO_2 emission solution (SOC(0) = 31 %, Capacity = 250 kWh).

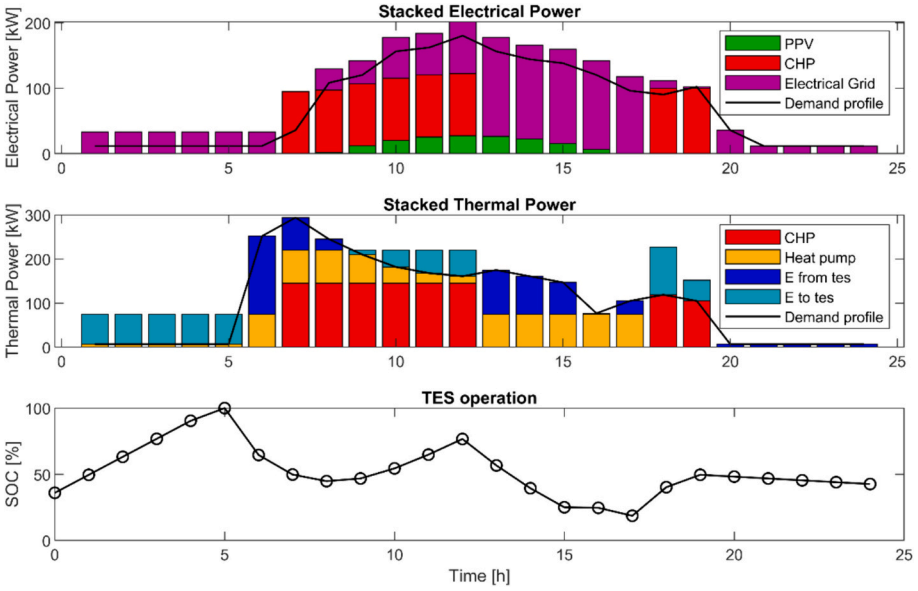

Fig. 12. Daily scheduling: heat pump for the optimal cost and optimal cost*CO_2 emission solutions (SOC(0) = 36 %, Capacity = 500 kWh).

storage sizing has been proposed and discussed. The main results of this work are summarized in the following point.

- The multi-objective optimization algorithm has been successfully implemented for the optimization of the proposed polygeneration grid including a T100 microturbine in CHP mode, 77 kW peak-power PV panels, a thermal energy storage device and a 150 kW boiler (option 1) or a 75 kW heat pump (option 2).
- The thermal energy storage optimization has been performed based on the proposed parametric curve plots. For the boiler case study, the result combination proposed 250 kWh hot water tank starting at 31 % SOC, while for the heat pump case a 500 kWh device and 36 % SOC at the simulation beginning.
- The hour-by-hour management results have shown few utilizations of the CHP for cost minimization (in the boiler case) against an important application of this microturbine for CO_2 emission minimization.
- The results have shown the benefits of the heat pump application for both costs and CO_2 emissions (−13.2 % cost decrease for the cost minimization case, −16.6 % CO_2 emission decrease for the CO_2 minimization case, and −35.2 % of cost*CO_2 for the case related to the minimization of this product).

CRediT authorship contribution statement

Mario Luigi Ferrari: Writing – review & editing, Writing – original draft, Supervision, Methodology, Investigation. **Lorenzo Gini:** Writing – review & editing, Writing – original draft, Visualization, Software, Investigation, Data curation. **Paolo Di Barba:** Supervision, Methodology, Conceptualization. **Maria Evelina Mognaschi:** Validation,

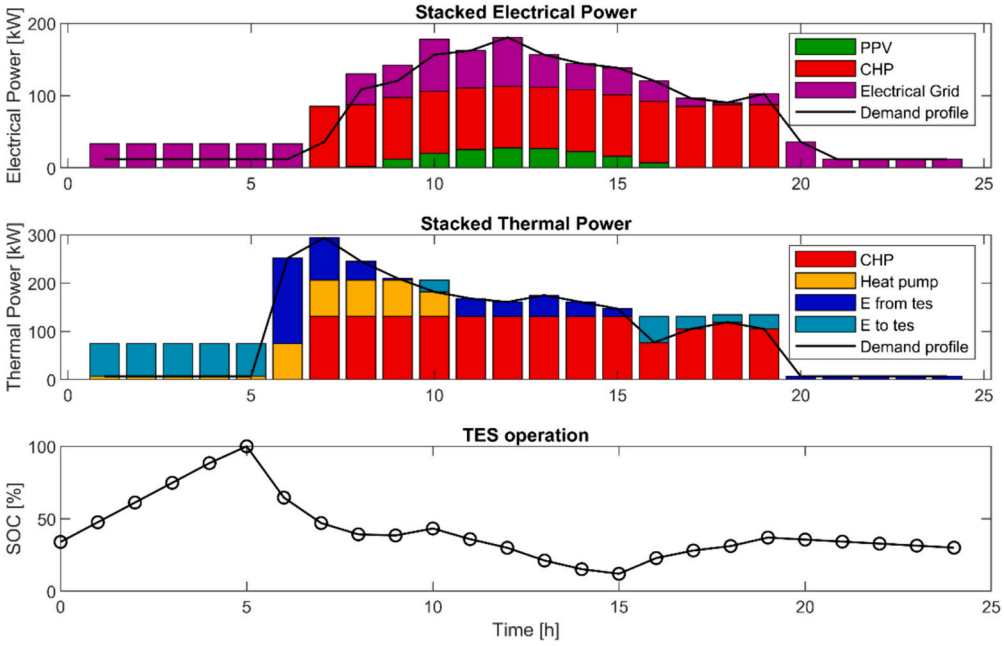

Fig. 13. Daily scheduling: heat pump for the optimal CO_2 emission solution (SOC(0) = 34 %, Capacity = 500 kWh).

Table 2
Summary of the global results.

	TES [kWh]	SOC(0) [%]	Costs [€]	CO_2 [kg]	Costs*CO_2 [€*kg]	Fig.
Boiler case	750	53	582.92	985.3	574,336.6	9
	750	12	766.02	750.2	574,651.1	10
	250	31	650.89	813.5	529,488.2	11
HP case	500	36	505.60	678.5	343,032.5	12
	500	34	635.38	625.3	397,273.4	13
	500	36	505.60	678.5	343,032.5	12

Software, Methodology, Formal analysis, Conceptualization. **Elisabetta Sieni:** Software, Methodology, Investigation, Conceptualization.

Declaration of competing interest

The authors declare that they have no known competing financial interests or personal relationships that could have appeared to influence the work reported in this paper.

Data availability

Data will be made available on request.

Acknowledgements

A special acknowledgement is reported for Francesco Sforzini, who supported the data analysis in his Bachelor thesis activities.

References

[1] A.N. Abdalla, M.S. Nazir, H. Tao, S. Cao, R. Ji, M. Jiang, L. Yao, Integration of energy storage system and renewable energy sources based on artificial intelligence: an overview, J. Energy Storage 40 (2021) (102811_1-13).
[2] X. Yu, Z. Li, Z. Zhang, L. Wang, G. Qian, R. Huang, X. Yu, Energy, exergy, economic performance investigation and multi-objective optimization of reversible heat pump-organic Rankine cycle integrating with thermal energy storage, J. Energy Storage 38 (2022) (102321_1-16).
[3] T. Reboli, M. Ferrando, L. Gini, L. Mantelli, A. Sorce, A. Traverso, Gas turbine combined cycle range enhancer – part 2: performance demonstration, J. Eng. Gas Turbines Power 144 (2022) (121013_1-11).
[4] A. Bouakkaz, A.J.G. Mena, S. Haddad, M.L. Ferrari, Efficient energy scheduling considering cost reduction and energy saving in hybrid energy system with energy storage, J. Energy Storage 33 (2021) (101887_1-13).
[5] https://www.arera.it/it/com_stampa/22/220929.htm.
[6] Y. Cui, Z. Geng, Q. Zhu, Y. Han, Review: multi-objective optimization methods and application in energy saving, Energy 125 (2017) 681–704.
[7] R. Kamal, F. Moloney, C. Wickramaratne, A. Narasimhan, D.Y. Goswami, Strategic control and cost optimization of thermal energy storage in buildings using EnergyPlus, Appl. Energy 246 (2019) 77–90.
[8] X. Zhang, R. Sharma, Y. He, Optimal Energy Management of a Rural Microgrid System Using Multi-objective Optimization, 2012 IEEE PES Innovative Smart Grid Technologies (ISGT), 2012, pp. 1–8.
[9] H.P. Benson, Multi-objective optimization: interactive methods for preference value functions, Encycl. Optimization (2008) 2471–2474.
[10] R. D'Souza, C. Sekaran, A. Kandasamy, Improved NSGA-II based on a novel ranking scheme, J. Comput. 2 (2010).
[11] K. Deb, H. Jain, An evolutionary many-objective optimization algorithm using reference-point-based nondominated sorting approach, part I: solving problems with box constraints, IEEE Trans. Evol. Comput. 18 (2014) 577–601.
[12] K. Deb, Multiobjective Optimization Using Evolutionary Algorithms, 1st ed., John Wiley and Sons, Chichester; New York, NY, 2001.
[13] J. Liu, C. Hu, A. Kimber, Z. Wang, Uses, cost-benefit analysis, and markets of energy storage systems for electric grid applications, J. Energy Storage 32 (2020) (101731_1-16).
[14] S. Barberis, M. Rivarolo, A. Traverso, A.F. Massardo, Thermo-economic analysis of the energy storage role in a real polygenerative district, J. Energy Storage 5 (2016) 187–202.
[15] S. Barberis, M. Rivarolo, A. Traverso, A.F. Massardo, Thermo-economic optimization of a real polygenerative district, Appl. Therm. Eng. 97 (2016) 1–12.
[16] S. Barberis, M. Rivarolo, D. Bellotti, L. Magistri, Heat pump integration in a real poly-generative energy district: a techno-economic analysis, Energ. Conver. Manage. X 15 (2022) (100238_1-10).
[17] M.L. Ferrari, A. Cuneo, M. Pascenti, A. Traverso, Real-time state of charge estimation in thermal storage vessels applied to a smart polygeneration grid, Appl. Energy 206 (2017) 90–100.
[18] S. Alqaed, Heating a residential building using the heat generated in the lithium ion battery pack by the electrochemical process, J. Energy Storage 45 (2022) (103553_1-16).
[19] M. Cavo, E. Gadducci, D. Rattazzi, M. Rivarolo, L. Magistri, Dynamic analysis of PEM fuel cells and metal hydrides on a zero-emission ship: a model-based approach, Int. J. Hydrogen Energy 46 (2021) 32630–32644.
[20] M. Rivarolo, G. Riveros-Godoy, L. Magistri, A.F. Massardo, Clean hydrogen and Ammonia synthesis in Paraguay from the Itaipu 14 GW hydroelectric plant, ChemEngineering 3 (2019) 1–11.
[21] G. Ferrer, C. Barreneche, A. Solé, I. Martorell, L.F. Cabeza, New proposed methodology for specific heat capacity determination of materials for thermal energy storage (TES) by DSC, J. Energy Storage 11 (2017) 1–6.
[22] T. Reboli, M. Ferrando, A. Traverso, J.N.W. Chiu, Thermal energy storage based on cold phase change materials: charge phase assessment, Appl. Therm. Eng. 217 (2022) (119177_1-12).
[23] A. De Gracia, L.F. Cabeza, Phase change materials and thermal energy storage for buildings, Energ. Buildings 103 (2015) 414–419.

[24] X. Zhou, M. Mahmood, J. Chen, T. Yang, G. Xiao, M.L. Ferrari, Validated model of thermochemical energy storage based on cobalt oxides, Appl. Therm. Eng. 159 (2019) (113965_1–14).
[25] A. Gil, M. Medrano, I. Martorell, A. Lázaro, P. Dolado, B. Zalba, L.F. Cabeza, State of the art on high temperature thermal energy storage for power generation. Part 1 - concepts, materials and modellization, Renew. Sustain. Energy Rev. 14 (2010) 31–55.
[26] J. Vivian, P. Heer, M. Fiorentini, Optimal sizing and operation of seasonal ice thermal storage systems, Energ. Buildings 3001 (2023) 113633.
[27] C.S.M. Nakama, B.R. Knudsen, A.C. Tysland, A simple dynamic optimization-based approach for sizing thermal energy storage using process data, Energy 2681 (2023) 126671.
[28] C. Pan, N. Vermaak, X. Wang, C. Romero, S. Neti, C.-H. Chen, R. Bonner, A fast dynamic model for a large scale heat pipe embedded latent heat thermal energy storage system for optimal sizing and control, J. Energy Storage 51 (2022) 104489.
[29] M.L. Ferrari, A. Traverso, A.F. Massardo, Smart polygeneration grids: experimental performance curves of different prime movers, Appl. Energy 162 (2016) 622–630.
[30] A. Traverso, TRANSEO code for the dynamic performance simulation of micro gas turbine cycles, in: ASME Paper GT2005-68101, 2005.
[31] S. Barberis, M. Rivarolo, D. Bellotti, L. Magistri, Heat pump integration in a real poly-generative energy district: a techno-economic analysis, Energ. Conver. Manage. X 15 (2022) (100238_1-10).
[32] A. Cuneo, A. Greco, M. Rivarolo, A.F. Massardo, Design optimization of smart poly generation grids through a model based approach, in: Proceedings of ECOS 2014, June 15-19, Turku, Finland, 2014.
[33] C. Torti, L. Magistri, A.F. Massardo, Development of time dependent calculation tools for plant operating optimization, Paper EFC09-17109, in: 3rd European Fuel Cell technology and Application Conference, 2009.
[34] K. Miettinen, Nonlinear Multiobjective Optimization vol. 12, Springer Science & Business Media, 1999.
[35] P. Di Barba, Multiobjective Shape Design in Electricity and Magnetism, Springer, 2010.
[36] P. Di Barba, M.E. Mognaschi, L. Petkovska, G.V. Cvetkovski, Optimal shape design of a class of permanent magnet motors in a multiple-objectives context, COMPEL – Int. J. Comput. Math. Electric. Electron. Eng. 41 (2022) 1994–2009.
[37] P. Di Barba, M.E. Mognaschi, E. Sieni, Many objective optimization of a magnetic micro-electro-mechanical (MEMS) micromirror with bounded MP-NSGA algorithm, Mathematics 8 (2020) 1509.
[38] P. Di Barba, M.E. Mognaschi, S. Wiak, A non-differential method for solving many-objective optimization problems: an application in IPM motor design, Int. J. Appl. Electromagn. Mech. 64 (2020) S131–S142.
[39] A. Shaban, H. Maher, M. Elbayoumi, S. Abdelhady, A cuckoo load scheduling optimization approach for smart energy management, Energy Rep. 7 (2021) 4705–4721.
[40] S. Ali, K. Ullah, G. Hafeez, I. Khan, F.R. Albogamy, S.I. Haider, Solving day-ahead scheduling problem with multi-objective energy optimization for demand side management in smart grid, Eng. Sci. Technol. Int. J. 36 (2022) 101135.
[41] N. Javaid, S. Javaid, W. Abdul, I. Ahmed, A. Almogren, A. Alamri, I.A. Niaz, A hybrid genetic wind driven heuristic optimization algorithm for demand side management in smart grid, Energies 10 (2017) 1–27.
[42] J. Du, Z. Zhang, M. Li, J. Guo, K. Zhu, Optimal scheduling of integrated energy system based on improved grey wolf optimization algorithm, Sci. Rep. 12 (2022) 1–19.
[43] K.S. Reddy, L.K. Panwar, R. Kumar, B.K. Panigrahi, Distributed resource scheduling in smart grid with electric vehicle deployment using fireworks algorithm, J. Mod. Power Syst. Clean Energy 4 (2016) 188–199.
[44] https://unigesostenibile.unige.it/smart_grid_savona.
[45] https://re.jrc.ec.europa.eu/pvg_tools/en/tools.html#MR.
[46] https://www.arera.it/allegati/docs/21/483-21.pdf.